Substrate stiffness regulates solubility of cellular vimentin

Maria E. Murray[a,b], Melissa G. Mendez[b], and Paul A. Janmey[b]
[a]Department of Bioengineering and [b]Institute for Medicine and Engineering, University of Pennsylvania, Philadelphia, PA 19104

ABSTRACT **The intermediate filament protein vimentin is involved in the regulation of cell behavior, morphology, and mechanical properties. Previous studies using cells cultured on glass or plastic substrates showed that vimentin is largely insoluble. Although substrate stiffness was shown to alter many aspects of cell behavior, changes in vimentin organization were not reported. Our results show for the first time that mesenchymal stem cells (hMSCs), endothelial cells, and fibroblasts cultured on different-stiffness substrates exhibit biphasic changes in vimentin detergent solubility, which increases from nearly 0 to 67% in hMSCs coincident with increases in cell spreading and membrane ruffling. When imaged, the detergent-soluble vimentin appears to consist of small fragments the length of one or several unit-length filaments. Vimentin detergent solubility decreases when these cells are subjected to serum starvation, allowed to form cell–cell contacts, after microtubule disruption, or inhibition of Rac1, Rho-activated kinase, or p21-activated kinase. Inhibiting myosin or actin assembly increases vimentin solubility on rigid substrates. These data suggest that in the mechanical environment in vivo, vimentin is more dynamic than previously reported and its assembly state is sensitive to stimuli that alter cellular tension and morphology.**

Monitoring Editor
Thomas M. Magin
University of Leipzig

Received: Jun 19, 2013
Revised: Oct 23, 2013
Accepted: Oct 25, 2013

INTRODUCTION

The responses of cells to the mechanical properties of the substrate to which they adhere varies as widely as their response to chemical signals and include modulation of cell spreading (Pelham and Wang, 1997), motility (Pelham and Wang, 1997; Raab *et al.*, 2012), transcription (Dupont *et al.*, 2011), proliferation (Klein *et al.*, 2009), and differentiation (Engler *et al.*, 2004b, 2006). These changes are especially well-characterized in human mesenchymal stem cells (hMSCs). Control of substrate stiffness alone is sufficient to drive hMSCs to differentiate into mature adipocytes or osteocytes in differentiation-permissive medium (Engler *et al.*, 2006) or to induce quiescence in cells maintained in growth medium on soft substrates (Winer *et al.*, 2009a).

Studies of cell responses to substrate mechanical properties often focus on actin-related cytoskeletal components (Rotsch and Radmacher, 2000). Actin polymerization and stress fiber formation are generally enhanced by stiffer substrates, and these features contribute to the cortical stiffening that accompanies cell spreading on stiff substrates (Solon *et al.*, 2007; Byfield *et al.*, 2009; Tee *et al.*, 2011). Vimentin networks also have physical properties likely to contribute to cell mechanics, characterized by a high degree of strain stiffening and ability to withstand large strains without breakage (Kreplak *et al.*, 2005; Qin *et al.*, 2009), in contrast to microtubules and microfilaments, which rupture at more moderate strains (Janmey *et al.*, 1991). The relative stability and compliance of intermediate filament (IF) networks to large strains suggest that the vimentin network of mesenchymal cells might be important for the mechanical integrity of these cells in vivo.

Unlike the soluble pools of G-actin and tubulin dimers necessary to maintain the ongoing exchange of subunits with F-actin or microtubules, respectively, IF in cultured cells maintain only a tiny (~1–3%) soluble fraction, as determined by ultracentrifugation followed by chromatography (Soellner *et al.*, 1985) or by detergent fractionation (Osborn and Weber, 1977; Blikstad and Lazarides, 1983; Gilbert and Fulton, 1985). The soluble fraction of vimentin after ultracentrifugation contains solutes of the size of vimentin tetramers or smaller

This article was published online ahead of print in MBoC in Press (http://www.molbiolcell.org/cgi/doi/10.1091/mbc.E13-06-0326) on October 30, 2013.

Address correspondence to: Maria E. Murray (murrayma@seas.upenn.edu).

Abbreviations used: AFM, atomic force microscopy; hMSC, human mesenchymal stem cell; HUVEC, human umbilical vein endothelial cells; IF, intermediate filaments; MT, microtubule; PAK, p21-activated kinase; ROCK, Rho-activated kinase.

oligomers, but larger vimentin assemblies such as the unit length filament (ULF; Strelkov *et al.*, 2003) proposed to be an essential intermediate of IF assembly would also be released into a detergent-soluble fraction before ultracentrifugation.

When cells containing IF are cultured on glass and subjected to detergent lysis, the detergent-soluble IF pool is small compared with the fraction that remains within the insoluble cytoskeletal fraction (Blikstad and Lazarides, 1983; Hinz *et al.*, 2003), consistent with the results generated by solubility data from sedimentation studies (Soellner *et al.*, 1985). A condition of all of the experiments used to generate previous data, however, was the use of glass or tissue culture plastic substrates, the stiffnesses of which are orders of magnitude greater than those of tissues in vivo (Levental *et al.*, 2007).

Here we examine vimentin assembly in cells grown on substrates of physiologically relevant elastic moduli. On these substrates, a large fraction of vimentin becomes Triton soluble, and the balance between soluble and insoluble vimentin shifts in a substrate stiffness-dependent manner. This balance is sensitive to perturbations of actin, microtubules, and signaling intermediates that alter intracellular tension.

RESULTS

Vimentin organization in cells on soft substrates

To determine whether substrate mechanics alter vimentin organization, we examined vimentin networks in hMSCs cultured on different stiffness fibronectin-coated polyacrylamide gels by fluorescence microscopy. On 0.2-kPa gels, similar to the stiffness of bone marrow and adipose tissue, vimentin networks surround the nucleus, as is characteristic (Figure 1, I and M). Actin stress fibers are not evident (Figure 1E). On 5-kPa gels, vimentin networks fill 63% of the cytoplasmic region, extending from the nucleus but not reaching the cell periphery (Figure 2D). These cells are elongated (Figure 1B), and 70% display actin-containing ruffles (Figure 2E; arrow in inset indicates ruffle). The vimentin network in cells cultured on 30-kPa gels fills 78% of the cytoplasmic region, and fewer cells (21%) exhibit ruffling edges (Figure 2E, inset). Under these conditions, actin fibers are evident (Figure 1, G and H).

The substrate stiffness dependence of cell spread area and aspect ratio has been shown for a variety of cell types (Pelham and Wang, 1997; Engler *et al.*, 2004a; Winer *et al.*, 2009a). In hMSCs, spread area increases with substrate stiffness, whereas aspect ratio increases to a maximum at 10 kPa and then decreases (Figure 2A). Human umbilical vein endothelial cells (HUVECs) also increase in spread area as the substrate stiffness increases (Figure 2B), and the aspect ratio peaks at 30 kPa before decreasing slightly (Figure 2B). 3T3 cells increase both spread area and aspect ratio monotonically with substrate stiffness (Figure 2C).

Substrate stiffness regulates vimentin organization

Vimentin networks are apparent in cells on substrates of all stiffnesses, and the organization of these networks varies with substrate stiffness (Figures 1 and 2). To determine whether this results from changes in vimentin protein levels, we prepared immunoblots of whole-cell lysates. The amount of vimentin is consistent across all conditions (Figure 2, F and G).

To further quantify substrate stiffness–dependent changes in vimentin organization or assembly, we prepared Triton-soluble and -insoluble fractions. Fractionation by Triton extraction revealed striking, biphasic changes in the proportions of the detergent-soluble and -insoluble fractions. In hMSCs (Figure 3, A and B) and HUVECs (Figure 3, C and D), little vimentin partitions into the detergent-soluble fraction when cells are grown on the softest gel (0.2 kPa; hMSCs, 3 ±1%; HUVECs, 29 ±21%). This fraction increases significantly in cells grown on 5-kPa substrates (hMSCs, 67 ±6%; HUVECs, 68 ±15%). On stiffer substrates, the proportion of detergent-soluble vimentin decreases, and cells grown on fibronectin-coated silanized glass contain detergent-soluble fractions consistent with those demonstrated by previous studies (hMSCs, 2 ±1%; HUVECs, 19 ±10%). The vimentin in NIH-3T3 cells partitions similarly and shows the greatest detergent-soluble pool at 30 kPa (Figure 3, E and F; 30 kPa, 46 ±10%).

Assembly state of detergent-soluble vimentin

To assess the assembly state of the soluble vimentin pool in cells cultured on soft substrates, we centrifuged Triton-soluble fractions at low speed (3000 × g, 10 min; Eriksson *et al.*, 2004). The bulk of vimentin detectable by Western blotting partitioned into the low-speed pellet (Figure 4A). This result shows that the Triton-soluble vimentin fraction is composed of small filaments or other aggregates rather than vimentin dimers or tetramers.

Detergent-soluble vimentin was imaged using atomic force microscopy (AFM) in order to determine the length of the detergent-soluble filaments (Figure 4). The detergent-soluble fraction that sedimented after centrifugation was resuspended in sodium phosphate buffer and adsorbed to a mica support, and the dried sample was imaged. No structures resembling long IFs or any other cytoskeletal filament were observed in these preparations. The largest structures that were evident were short filaments with an apparent diameter of 30–40 nm, similar to the size of purified vimentin filaments prepared and imaged under similar conditions (Ando *et al.*, 2004; Mücke *et al.*, 2005). The average filament length was 118 ± 43 nm (SD), with a range from 60 to 230 nm (Figure 4B). The filaments also have a characteristic beaded appearance with a period of 28 ± 5 nm (SD; Figure 4, C–K), which has also been reported for purified vimentin IFs imaged by AFM but is not observed with F-actin (Weisenhorn *et al.*, 1990) or microtubules (Kacher *et al.*, 2000). These filament lengths are on the order of one to several unit-length filaments, which were previously measured as 60–80 nm (Mücke *et al.*, 2005) or 78 nm in length (Ando *et al.*, 2004) using purified vimentin.

Vimentin detergent solubility and cytoskeletal cross-talk

Intermediate filament networks interact with the actin and microtubule networks to regulate cell behavior (Chang and Goldman, 2004). To determine whether cytoskeletal contractility or different cytoskeletal components affect vimentin organization on soft substrates, we perturbed these systems and monitored cells for changes in vimentin organization (Figure 5; summarized in Table 1).

Because vimentin interacts with microtubules (MTs) directly (Bocquet *et al.*, 2009) and in both a kinesin-dependent (Gyoeva and Gelfand, 1991) and dynein-dependent (Helfand *et al.*, 2002) manner, we examined whether the perturbation of MTs would alter the detergent-soluble vimentin fraction. In hMSCs plated on 5-kPa gels, either nocodazole or Taxol treatment decreased the fraction of detergent-soluble vimentin (Figure 5). On the 30-kPa gels, however, perturbation of MTs did not change vimentin detergent solubility. Following immunofluorescence staining and imaging, the vimentin and microtubule networks appear in the control cells on both soft and stiff substrates (Supplemental Figure S1, A–D). When treated with nocodazole, the microtubule network disassembles (Figure 6, F and H), whereas the vimentin network appears unchanged (Supplemental Figure S1, E and G). The negative spaces in the 30-kPa nocodazole-treated vimentin image reflect the presence of actin stress fibers (Supplemental Figure S1G). After Taxol treatment, microtubules are

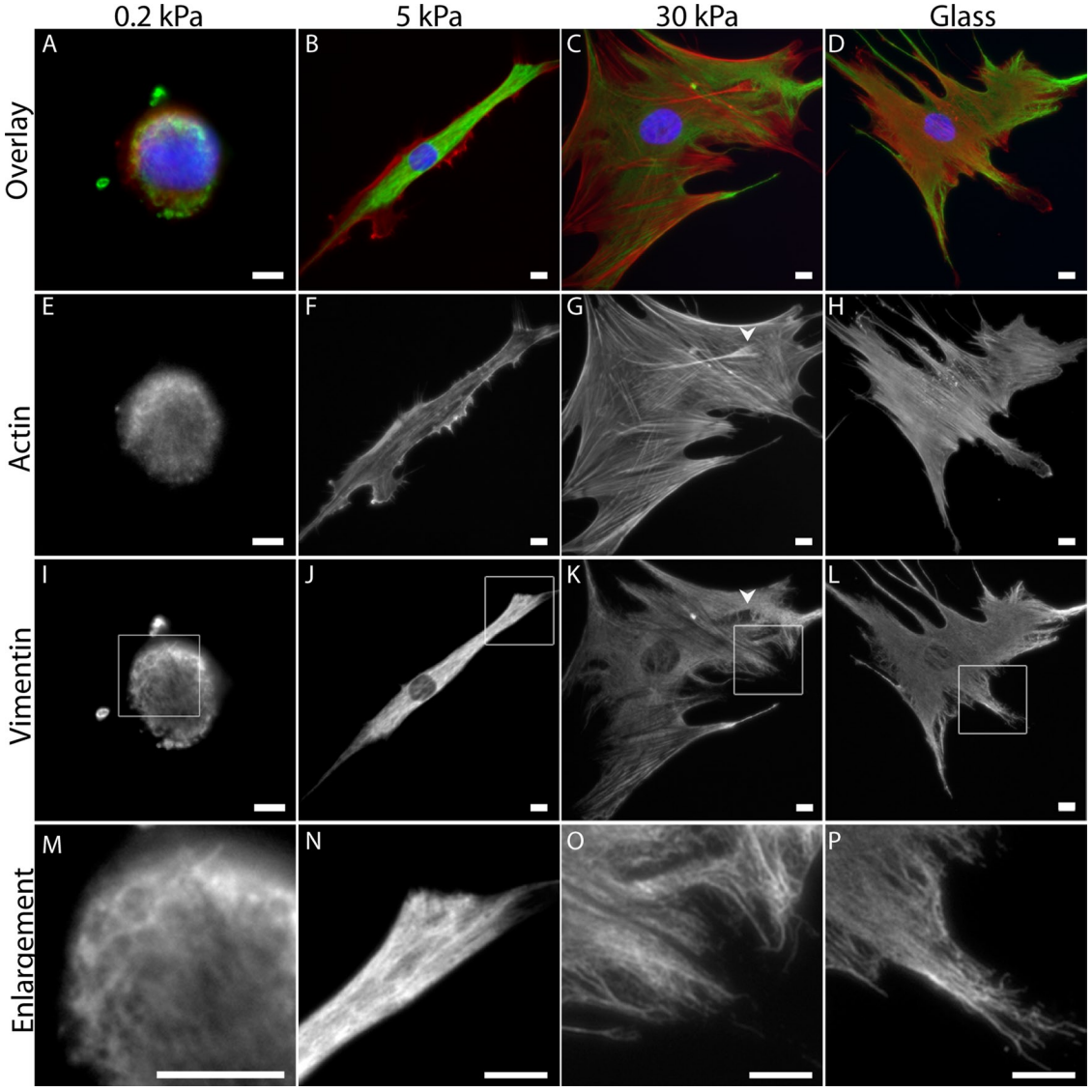

FIGURE 1: Vimentin in hMSCs on different-stiffness gels. Vimentin networks are evident in cells on gels over a wide range of stiffnesses (A–D; actin, red; vimentin, green; and nuclei, blue). On 0.2-kPa gels hMSCs are small and round (Figure 2, A, E, I, and M). Cells elongate on 5-kPa gels (B, F, J, N). On 30-kPa gels and silanized glass, cells spread similarly and contain stress fibers (G, H), and the vimentin network extends to the cell edge (O, P). Bars, 10 μm.

stabilized (Supplemental Figure S1, J and L), and the vimentin network looks similar (Supplemental Figure S1, I and K).

Drug-induced MT depolymerization activates the RhoA pathway (Liu *et al.*, 1998), which might indirectly affect cell contractility, as seen previously in hMSCs (Winer *et al.*, 2009b). To assess the extent to which this might contribute to the nocodazole-induced vimentin solubility decrease, we treated cells with nocodazole and blebbistatin together. When cells on a 5-kPa gel are treated with both agents, vimentin detergent solubility decreased to an extent similar to that seen after nocodazole treatment alone, suggesting that the nocodazole-induced decrease in vimentin solubility results from the loss of MTs rather than RhoA-dependent myosin activation. On 30-kPa gels, the combined treatment had no effect. Under immunofluorescence for vimentin (Supplemental Figure S2, M and O) and actin (Supplemental Figure S2, N and P), cells appear to have altered their shape, while vimentin filaments are still seen.

Actomyosin contractility changes in cells grown on different substrates in a myosin II–dependent manner (Even-Ram *et al.*, 2007). To determine whether actomyosin contractility contributes to the changes in vimentin organization evident in cells on gel substrates, we treated cells with either the myosin II inhibitor blebbistatin or the actin polymerization inhibitor cytochalasin D. In cells cultured on 5-kPa substrates, neither blebbistatin nor cytochalasin D alters vimentin detergent solubility. In cells cultured on 30-kPa gels, however, the proportion of detergent-soluble vimentin increases after blebbistatin or cytochalasin D treatment. After blebbistatin treatment, actin stress fibers disappear, retraction fibers are seen (Supplemental Figure S2, F and H), and the vimentin network does not look different (Supplemental Figure S2, E and G).

Finally, serum starvation is another way to decrease migration and cytoskeletal dynamics. In fibroblasts, serum starvation causes the vimentin network to extend to the edge of the cell coincident with the loss of ruffling (Helfand *et al.*, 2011). To determine whether

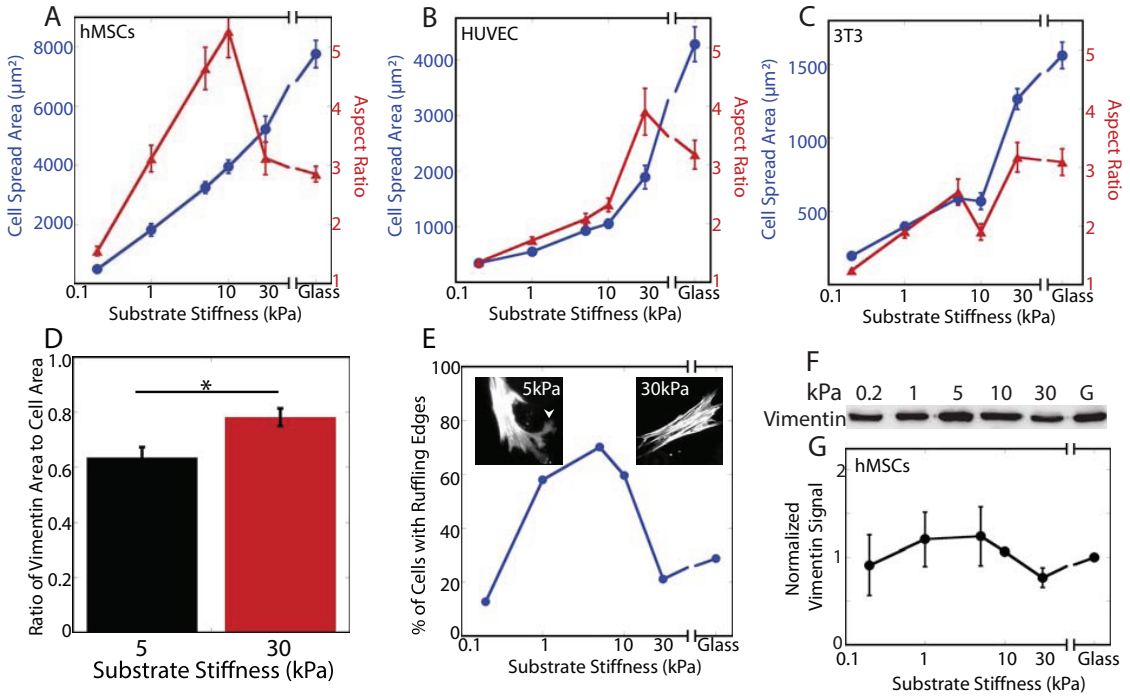

FIGURE 2: Substrate stiffness causes changes in spread area, aspect ratio, and ruffling behavior but not total vimentin protein by whole-cell lysis. In all cell types tested, spread area increases with substrate stiffness (A–C; blue), whereas the aspect ratio peaks and then decreases in hMSCs (A; red) and HUVECs (B; red) but not 3T3 cells (C; red). The vimentin network extends to fill a greater proportion of the cell on stiffer substrates (D; 5 kPa, 63 ± 10% vs. 30 kPa, 78 ± 3%; $p < 0.05$; see also Figure 4, A–D). Changes in ruffling behavior also accompany substrate stiffness changes (E; arrowhead in left inset indicates a ruffling edge; compare to nonruffling cell, right inset; F-actin staining). Total vimentin expression is not altered by substrate stiffness (F, G; $p > 0.1$ across all conditions).

changes in vimentin detergent solubility accompany these changes, we serum starved cells on 5- and 30-kPa gels for 5 d. Consistent with previous results, the removal of serum causes the vimentin network to reorganize toward the cell edge as ruffling is abrogated (Supplemental Figure S2, U–X). Under this condition, the Triton-soluble fraction of vimentin decreases in cells grown on 5-kPa, but not 30-kPa, gels (Figure 5).

Substrate-dependent effect of Rho-family GTPases

The effects of actomyosin inhibition described here implicate kinases involved in the RhoA and Rac1 signal transduction cascades (Figure 6A). Kinases that are activated by these pathways can phosphorylate vimentin and have known roles in mechanotransduction. In cells on 5-kPa gels, inhibition of Rho-activated kinase (ROCK) or Rac activation decreases vimentin detergent solubility (Figure 6; summarized in Table 1). In contrast, ROCK or Rac inhibition *increases* vimentin solubility in cells grown on 30-kPa gels. Inhibition of p21-activated kinase (PAK; by IPA-3), which is downstream of Rac1, decreases vimentin solubility in cells cultured on 5-kPa gels but not in cells grown on 30-kPa gels.

DISCUSSION

In contrast to the results of previous studies showing that nearly all cellular vimentin exists in an insoluble filamentous form, the results here show that on substrates with stiffnesses in the physiological range, as much as 67% of the vimentin is released upon detergent lysis. The size of this pool varies with substrate stiffness and is further modulated by intracellular signals that affect actin and microtubule assembly and internal tension. It is unlikely that this pool consists of vimentin dimers or tetramers because the detergent-soluble fraction sediments at low centrifugal forces. AFM reveals that the vimentin-detergent soluble pool consists of filaments that are the length of one or several unit-length filaments. Although ULFs have been formed in experiments with purified vimentin, their involvement in IF assembly in vivo is not yet established. However, the data of Figure 4 suggest that structures similar to those predicted for ULFs can be isolated from cells.

These studies show that the assembly state of vimentin, like that of actin, is strongly dependent on the mechanical environment of the cell and responds to changes in substrate stiffness. Cytoskeletal-dependent cell characteristics such as motility (Peyton and Putnam, 2005), shape (Yeung *et al.*, 2005), and contractility (Califano and Reinhart-King, 2010) that have been shown to depend on substrate stiffness might therefore be affected by changes in IF assembly state, as well as by changes in other cytoskeletal elements. Because substrate stiffness affects Rho-family GTPase signaling (Bhadriraju *et al.*, 2007; Klein *et al.*, 2009) and inhibition of ROCK or Rac activation alters cellular vimentin assembly, kinases that are regulated by GTPases and that phosphorylate vimentin (Hyder *et al.*, 2008) might be essential for the greater solubility of vimentin on substrates with physiologically relevant stiffness.

The two main signaling pathways implicated in both mechanosensing and the regulation of the vimentin network are the RhoA and Rac pathways. RhoA activity decreases with decreasing substrate stiffness (Kim *et al.*, 2009), which in turn diminishes ROCK activity (Bhadriraju *et al.*, 2007). Phosphorylation of vimentin at S38 and S72 by ROCK prevents vimentin polymerization in vitro (Goto *et al.*, 1998) and depolymerizes vimentin in cells (Eriksson *et al.*, 2004). Therefore it is plausible that the reduction in RhoA activity caused by cell growth on a substrate with physiological-range

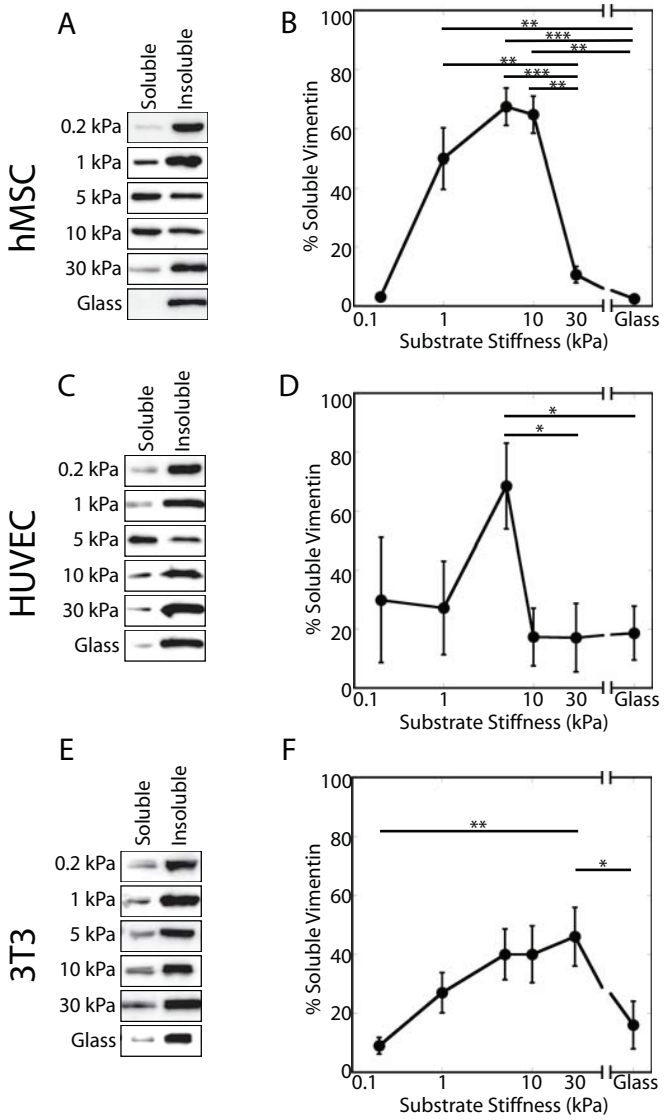

FIGURE 3: Detergent-soluble vimentin varies with substrate stiffness. The soluble and insoluble fractions of vimentin in hMSCs, HUVECs, and NIH-3T3 cells vary with substrate stiffness. In all cell types tested, vimentin solubility exhibits a biphasic response characterized by a small soluble pool on the softest substrates, which increases with substrate stiffness until peaking at 5 kPa (A, B, hMSCs; C, D, HUVECs) or 30 kPa (E, F; NIH-3T3 cells).

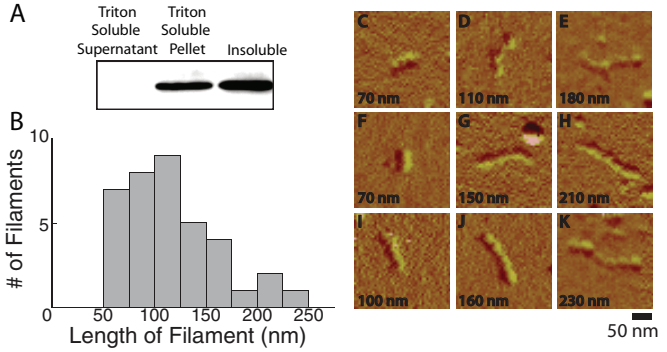

FIGURE 4: Detergent solubility and vimentin assembly state. To understand the differences between detergent-soluble vimentin and soluble vimentin as determined by centrifugation, the detergent-soluble vimentin pool was centrifuged at 3000 × *g* for 10 min. Detergent-soluble vimentin pellets at low speeds when subjected to low-speed centrifugation (A). Quantification showed ($n = 3$) that 65% of the vimentin was present in the low-detergent pellet, with 3% of the vimentin in the low-detergent supernatant and the majority of the protein in the soluble fraction. The length of the filaments in the detergent-soluble pool was determined by imaging the filaments with AFM (B). Filaments demonstrate a beaded morphology and a diameter similar to previously observed results for vimentin (C–K).

stiffness could lead to a downstream change in vimentin assembly. This hypothesis is supported by the difference between ROCK inhibition (Y-27632) and contractility reduction (blebbistatin) on 5-kPa substrates. ROCK inhibition, which blocks both contractility and phosphorylation, results in a decrease in the detergent-soluble vimentin pool. Blebbistatin treatment results in no change in the amount of detergent-soluble vimentin. Taken together, these data suggest that kinase activity is necessary for the maintenance of the detergent-soluble vimentin pool.

The FAK-Rac-PAK pathway also responds to mechanical signals and is important in vimentin network disassembly. FAK phosphorylation facilitates Rac activation (Chang and Lemmon, 2007). Rac-GTP then activates PAK and alters cytoskeletal dynamics (Edwards *et al.*, 1999). PAK phosphorylates vimentin (Goto *et al.*, 2002), and PAK phosphorylation of vimentin$^{Ser\text{-}56}$ causes network disassembly (Li *et al.*, 2006). We show that Rac inhibition decreases soluble vimentin in cells grown on 5-kPa gels, a result that could be caused by the loss of PAK activation and consequent stabilization of the vimentin network. Serum starvation also decreases Rac signaling (Ridley and Hall, 1992), and Figure 5 shows that detergent-soluble vimentin also decreases when cells on 5-kPa gels are starved for serum.

Conclusions

By controlling the mechanical environment of the cell and perturbing specific signals that alter cell morphology, the work reported here shows that, in contrast to results from earlier studies on rigid substrates, a large fraction of the vimentin intermediate filament protein in hMSCs, HUVECs, and 3T3 cells becomes detergent

	On 5-kPa gels (%)	On 30-kPa gels (%)
Control	67 ± 6	11 ± 3
Blebbistatin	72 ± 3	32 ± 7
Cytochalasin D	71 ± 13	27 ± 10
Nocodazole	31 ± 7	9 ± 8
Taxol	24 ± 12	9 ± 7
Nocodazole + blebbistatin	24 ± 4	8 ± 3
Confluent monolayer	3 ± 3	2 ± 1
Serum starvation	15 ± 2	10 ± 8
Y-27632 (ROCK inhibition)	39 ± 6	35 ± 6
NSC23766 (Rac1 inhibition)	45 ± 4	36 ± 7
IPA-3 (PAK inhibition)	24 ± 9	25 ± 7

Red-shaded boxes indicate significant decrease from control of same stiffness, and green-shaded boxes indicate significant increase from control gel of same stiffness.

TABLE 1: Percentage of detergent-soluble vimentin under different treatment conditions.

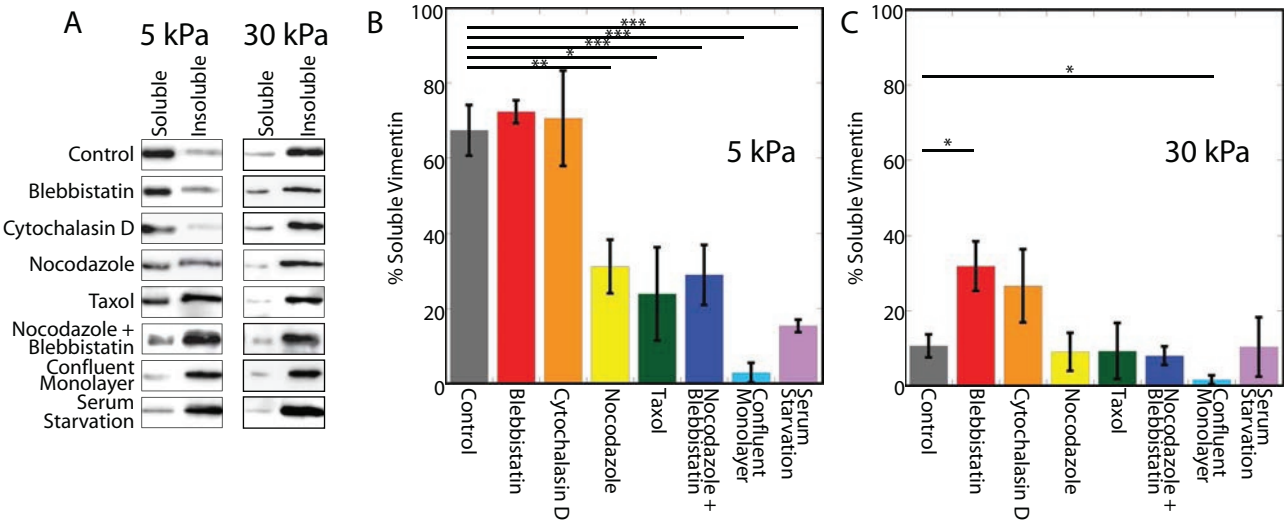

FIGURE 5: Changes in cytoskeletal organization affect vimentin detergent solubility in hMSCs. Perturbing microtubules decreases the amount of detergent-soluble vimentin in cells on 5-kPa but not 30-kPa gels (A, B; nocodazole, Taxol). In contrast, inhibiting myosin activity or actin assembly increases vimentin detergent solubility in cells on 30-kPa gels (A, C; blebbistatin, cytochalasin D). Inhibiting myosin activity in the presence of depolymerized MT does not compound the effect of MT depolymerization alone (compare nocodazole + blebbistatin to nocodazole).

soluble, but the total protein amount remains constant. The detergent-soluble vimentin pool does not consist primarily of vimentin dimers or tetramers, and AFM imaging of this fraction reveals short filaments with width and longitudinal spacing consistent with those of purified vimentin polymers. The length distribution of these structures suggests that they consist of one or several ULFs. The detergent-soluble fraction is maximal in cells grown on 5-kPa gels for hMSCs and HUVECs and 30-kPa gels in 3T3 cells and correlates strongly with the extent of cell ruffling and at least partially with axial ratio (Figure 2). Microtubules and serum are necessary to maintain vimentin solubility, whereas actin disruption has no effect on a 5-kPa substrate. When cells are grown on 30-kPa substrates, perturbation of cell contractility increases the detergent-soluble pool, whereas perturbing microtubules or removing serum has no effect. Culturing hMSCs in a confluent monolayer decreases the detergent-soluble pool on both soft and stiff substrates. Inhibiting ROCK or Rac decreases vimentin detergent solubility on 5-kPa gels but increases detergent solubility on 30-kPa gels, whereas PAK inhibition decreases vimentin solubility on 5-kPa gels. The differences in vimentin modulation by cells on 5- and 30-kPa gels suggest that this regulation is sensitive to stiffnesses within the physiological range and therefore might be essential to maintain mechanical homeostasis in cells over the large range of forces they encounter in vivo.

MATERIALS AND METHODS

Cell culture

Human mesenchymal stem cells were obtained from Lonza (Walkersville, MD) and cultured in low-glucose DMEM with 10% heat-inactivated fetal bovine serum (FBS) as previously described (Winer *et al.*, 2009a). NIH-3T3 cells (American Type Culture Collection, Manassas, VA) were cultured in DMEM supplemented with 10% heat-inactivated bovine calf serum (BCS). Human umbilical vein epithelial cells (Lonza) were cultured in EGM-2 Bullet Kit medium (Lonza). Cells were maintained at 37°C and 5% CO_2. For most experiments, cells were subcultured so as to be ~20% confluent after 24 h. For experiments of monolayer conditions, cells were plated at high density and incubated for 48 h. In the serum-starved condition, cells were cultured for 5 d on the substrate without serum.

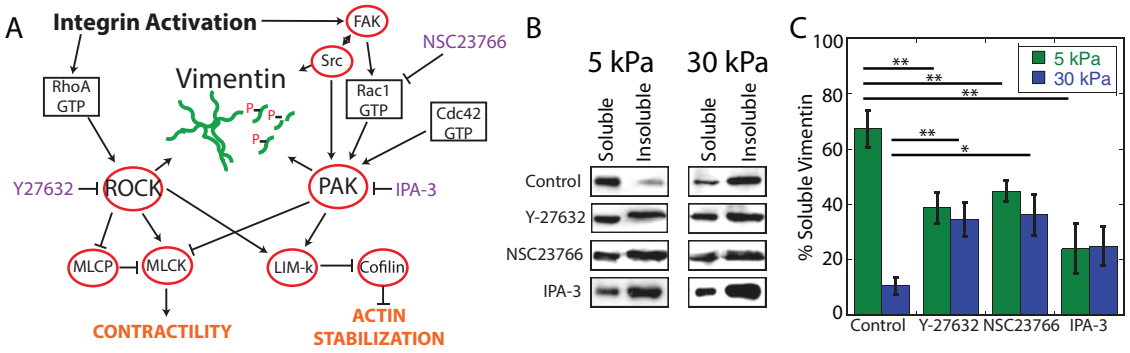

FIGURE 6: The effect of signaling inhibition on vimentin detergent solubility is substrate dependent. Both RhoA and Rac1 signaling are important in both mechanotransduction signaling and vimentin phosphorylation (A). ROCK (Y-27632) or Rac1 (NSC23766) inhibition decreases the proportion of detergent-soluble vimentin in cells on 5-kPa gels but increases it in cells on 30-kPa gels (B, C). Inhibiting PAK (IPA-3) decreases vimentin detergent solubility on 5-kPa gels but not on 30-kPa gels (B,C, comparison of control to IPA-3, $p = 0.088$).

Substrate fabrication

Cells were cultured on polyacrylamide gel substrates as described (Pelham and Wang, 1997; Yeung *et al.*, 2005). Briefly, solutions of 3.0% acrylamide and 0.06% bisacrylamide (0.2-kPa gel), 5.5% acrylamide and 0.1% bisacrylamide (1-kPa gel), 7.5% acrylamide and 0.2% bisacrylamide (5-kPa gel), 7.5% acrylamide and 0.3% bisacrylamide (10-kPa gel), or 12% acrylamide and 0.5% bisacrylamide (30-kPa gel) were prepared in 50 mM 4-(2-hydroxyethyl)-1-piperazineethanesulfonic acid (HEPES) buffer, pH 8, to a total volume of 500 ml. Gel stiffness is given as shear modulus (*G*′). Polymerization was initiated with *N*,*N*,*N*′,*N*′-tetramethylethylenediamine and ammonium persulfate. A 50-µl droplet was deposited on a 22-mm glass coverslip previously modified with 3-aminopropyltrimethoxysilane and glutaraldehyde. A 22-mm chlorosilanized coverslip was placed on top of the droplet and removed after polymerization was complete. The surface of the gels was functionalized by an ultraviolet-activating Sulfo-SANPAH (Thermo Fisher Scientific, Rockford, IL) cross-linker, and then the gels were submersed in fibronectin ligand (purified from human blood, 0.1 mg/ml in 50 mM HEPES) for a minimum of 2 h. Gels were then washed three times with phosphate-buffered saline (PBS), pH 7.4. Cells were plated on gels within 24 h of gel fabrication.

Immunofluorescence

Cells were fixed for immunofluorescence using 4% paraformaldehyde (room temperature, 10 min), permeabilized with 0.15% Triton X-100 for 5 min, and stained with primary antibody for 1 h. Cells were washed and stained with secondary antibody for 30 min. Stained preparations were imaged with a Hamamatsu (Hamamatsu, Japan) camera on a Leica DMIRE2 (Leica, Buffalo Grove, IL). Spread area and aspect ratio (ratio of the short axis to the long axis of the cell) were determined after tracing cell outlines (ImageJ, National Institutes of Health, Bethesda, MD). To determine the extent to which a vimentin network extended throughout a cell, we imaged the vimentin and actin networks and delineated the areas by comparing actin immunofluorescence (representative of the cell periphery) and vimentin immunofluorescence. Cells with ruffling membranes were defined as cells with areas of lobular membranes at the cell periphery.

Triton X-100–soluble extraction

Triton X-100 extraction of cells was performed as previously described, with minor modifications (Herrmann *et al.*, 2004). Briefly, gels were washed in PBS and inverted into a low-detergent buffer on ice (0.5× PBS, 50 mM 3-(*N*-morpholino)propanesulfonic acid, 10 mM $MgCl_2$, 1 mM ethylene glycol tetraacetic acid, and 0.15% Triton X-100 with 1 mM phenylmethanesulfonylfluoride, 50 mM sodium fluoride, and 1 mM sodium orthovanadate [all reagents from Sigma]) to permeabilize the cell membrane and release soluble protein. Insoluble protein was then extracted with 4× boiling Laemmli buffer. In one experiment, the soluble pool was spun down at low speed (3000 × *g*) in an Eppendorf centrifuge. The pellet was then resuspended in 4× boiling Laemmli buffer. Equal amounts were loaded on the SDS–PAGE gel.

SDS–PAGE and immunoblotting

For whole-cell lysis, cells were plated at low density and grown overnight. Before lysis, a minimum of 15 fields were imaged at low magnification and cells counted to allow loading of equal number of cells per lane. Cells were washed for 5 min in PBS and then inverted on Parafilm in a 50-µl droplet of 4× boiling Laemmli buffer for 5 min. Samples were then collected and boiled for 5 min before separation by SDS–PAGE and transfer to nitrocellulose membranes. The membranes were probed overnight in primary antibody in 5% milk before immunoblotting with horseradish peroxidase–conjugated secondary antibodies. Gels were imaged on a LAS-3000 (FujiFilm, Tokyo, Japan) using Amersham ECL Plus chemiluminescence (GE Healthcare, Piscataway, NJ). The protein band intensities were quantified using the Gel Analyzer module of ImageJ, and data were analyzed in Excel (Microsoft, Redmond, WA). Values of band intensity were normalized for each experiment to the intensity of the glass substrate band.

Antibodies and drug treatments

Antibodies included mouse monoclonal anti–vimentin V9 (Sigma-Aldrich, St. Louis, MO), chicken polyclonal anti-vimentin (Novus Biologicals, Littleton, CO), and mouse monoclonal anti–glyceraldehyde-3-phosphate dehydrogenase (Chemicon, Billerica, MA). Fluorophore-conjugated secondary antibodies were used for immunofluorescence (Jackson ImmunoResearch, West Grove, PA). Fluorophore-conjugated phalloidin was used to label polymerized actin (Molecular Probes, Eugene, OR). Cell nuclei were labeled with 4′,6-diamidino-2-phenylindole dihydrochloride (Sigma-Aldrich). For immunoblotting, peroxidase-conjugated secondary antibodies were used (GE Healthcare, Chalfont St Giles, United Kingdom). Cells were treated for 1 h with one or a combination of the following reagents (all from Sigma-Aldrich): blebbistatin (50 µM), cytochalasin D (1 µg/ml), nocodazole (1 µg/ml), Taxol (10 nM; Polioudaki *et al.*, 2009), Y-27632 (10 µM), NSC23766 (50 µM), and IPA-3 (in 10% dimethylsulfoxide, 10 µM). Controls were performed alongside each treatment and are presented in aggregate.

Atomic force microscopy

Atomic force microscopy was performed as previously described, with modifications (Ando *et al.*, 2004; Mücke *et al.*, 2005). Triton X-100 detergent–soluble fractions were collected from a 5-kPa gel and centrifuged in an Eppendorf tabletop centrifuge for 10 min at 3000 × *g*. The supernatant was discarded and the pellet resuspended in 2 mM sodium phosphate buffer, pH 7.5. The sample was then adsorbed to a freshly cleaved mica support for 10 min. The mica support was washed three times in deionized water and then dried. Samples were imaged on a NanoScope III atomic force microscope (Digital Instruments, Tonawanda, NY) in tapping mode with Au-coated silicon tip (Multi75GB; Ted Pella, Redding, CA).

Statistics

Results were tested for significant differences using two-tailed unpaired Student's *t* tests with equal variance. $p < 0.05$ were considered significant. In all figures, $*p < 0.05$; $**p < 0.01$, and $***p < 0.001$. All errors are given as SE of the results of at least three experimental repetitions, including a minimum of 45 cells/repetition.

ACKNOWLEDGMENTS

We acknowledge Yu-Hsiu Wang for assistance with atomic force microscopy. This work was supported by the National Institutes of Health (5F31AG041638 to M.E.M., 2T32HL007954 to M.E.M. and M.G.M., and 5P01GM096971 to P.A.J.).

REFERENCES

Ando S, Nakao K, Gohara R, Takasaki Y, Suehiro K, Oishi Y (2004). Morphological analysis of glutaraldehyde-fixed vimentin intermediate filaments and assembly-intermediates by atomic force microscopy. Biochim Biophys Acta 1702, 53–65.

Bhadriraju K, Yang M, Ruiz SA, Pirone DM, Tan J, Chen CS, Alom Ruiz S (2007). Activation of ROCK by RhoA is regulated by cell adhesion, shape, and cytoskeletal tension. Exp Cell Res 313, 3616–3623.

Blikstad I, Lazarides E (1983). Vimentin filaments are assembled from a soluble precursor in avian erythroid cells. J Cell Biol 96, 1803–1808.
Bocquet A, Berges R, Frank R, Robert P, Peterson AC, Eyer J (2009). Neurofilaments bind tubulin and modulate its polymerization. J Neurosci 29, 11043–11054.
Byfield FJ, Reen RK, Shentu T-P, Levitan I, Gooch KJ (2009). Endothelial actin and cell stiffness is modulated by substrate stiffness in 2D and 3D. J Biomech 42, 1114–1119.
Califano JP, Reinhart-King CA (2010). Substrate stiffness and cell area predict cellular traction stresses in single cells and cells in contact. Cell Mol Bioeng 3, 68–75.
Chang L, Goldman RD (2004). Intermediate filaments mediate cytoskeletal crosstalk. Nat Rev Mol Cell Biol 5, 601–613.
Chang F, Lemmon C (2007). FAK potentiates Rac1 activation and localization to matrix adhesion sites: a role for βPIX. Mol Biol Cell 18, 253–264.
Dupont S *et al*. (2011). Role of YAP/TAZ in mechanotransduction. Nature 474, 179–183.
Edwards DC, Sanders LC, Bokoch GM, Gill GN (1999). Activation of LIM-kinase by Pak1 couples Rac/Cdc42 GTPase signalling to actin cytoskeletal dynamics. Nat Cell Biol 1, 253–259.
Engler A, Bacakova L, Newman C, Hategan A, Griffin M, Discher D (2004a). Substrate compliance versus ligand density in cell on gel responses. Biophys J 86, 617–628.
Engler AJ, Griffin MA, Sen S, Bonnemann CG, Sweeney HL, Discher DE (2004b). Myotubes differentiate optimally on substrates with tissue-like stiffness: pathological implications for soft or stiff microenvironments. J Cell Biol 166, 877–887.
Engler AJ, Sen S, Sweeney HL, Discher DE (2006). Matrix elasticity directs stem cell lineage specification. Cell 126, 677–689.
Eriksson JE, He T, Trejo-Skalli AV, Härmälä-Braskén A-S, Hellman J, Chou Y-H, Goldman RD (2004). Specific in vivo phosphorylation sites determine the assembly dynamics of vimentin intermediate filaments. J Cell Sci 117, 919–932.
Even-Ram S, Doyle AD, Conti MA, Matsumoto K, Adelstein RS, Yamada KM (2007). Myosin IIA regulates cell motility and actomyosin-microtubule crosstalk. Nat Cell Biol 9, 299–309.
Gilbert M, Fulton AB (1985). The specificity and stability of the Triton-extracted cytoskeletal framework of gerbil fibroma cells. J Cell Sci 73, 335–345.
Goto H, Kosako H, Tanabe K, Yanagida M, Sakurai M, Amano M, Kaibuchi K, Inagaki M (1998). Phosphorylation of vimentin by Rho-associated kinase at a unique amino-terminal site that is specifically phosphorylated during cytokinesis. J Biol Chem 273, 11728–11736.
Goto H, Tanabe K, Manser E, Lim L, Yasui Y, Inagaki M (2002). Phosphorylation and reorganization of vimentin by p21-activated kinase (PAK). Genes Cells 7, 91–97.
Gyoeva F, Gelfand V (1991). Coalignment of vimentin intermediate filaments with microtubules depends on kinesin. Nature 353, 445–448.
Helfand BT *et al*. (2011). Vimentin organization modulates the formation of lamellipodia. Mol Biol Cell 22, 1274–1289.
Helfand BT, Mikami A, Vallee RB, Goldman RD (2002). A requirement for cytoplasmic dynein and dynactin in intermediate filament network assembly and organization. J Cell Biol 157, 795–806.
Herrmann H, Kreplak L, Aebi U (2004). Isolation, characterization, and in vitro assembly of intermediate filaments. Methods Cell Biol 78, 3–24.
Hinz B, Dugina V, Ballestream C, Wehrle-Haller B, Chaponnier C (2003). Alpha smooth muscle actin is crucial for focal adhesion maturation in myofibroblasts. Mol Biol Cell 14, 2508–2519.
Hyder CL, Pallari H-M, Kochin V, Eriksson JE (2008). Providing cellular signposts—post-translational modifications of intermediate filaments. FEBS Lett 582, 2140–2148.
Janmey PA, Euteneuer U, Traub P, Schliwa M (1991). Viscoelastic properties of vimentin compared with other filamentous biopolymer networks. J Cell Biol 113, 155–160.
Kacher CM, Weiss IM, Stewart RJ, Schmidt CF, Hansma PK, Radmacher M, Fritz M (2000). Imaging microtubules and kinesin decorated microtubules using tapping mode atomic force microscopy in fluids. Eur Biophys J 28, 611–620.
Kim TJ, Seong J, Ouyang M, Sun J, Lu S, Hong JP, Wang N, Wang Y (2009). Substrate rigidity regulates Ca2+ oscillation via RhoA pathway in stem cells. J Cell Physiol 218, 285–293.
Klein EA, Yin L, Kothapalli D, Castagnino P, Byfield FJ, Xu T, Levental I, Hawthorne E, Janmey PA, Assoian RK (2009). Cell-cycle control by physiological matrix elasticity and in vivo tissue stiffening. Curr Biol 19, 1511–1518.
Kreplak L, Bär H, Leterrier JF, Herrmann H, Aebi U (2005). Exploring the mechanical behavior of single intermediate filaments. J Mol Biol 354, 569–577.
Levental I, Georges PC, Janmey PA (2007). Soft biological materials and their impact on cell function. Soft Matter 3, 299–306.
Li Q-F, Spinelli AM, Wang R, Anfinogenova Y, Singer HA, Tang DD (2006). Critical role of vimentin phosphorylation at Ser-56 by p21-activated kinase in vimentin cytoskeleton signaling. J Biol Chem 281, 34716–34724.
Liu B, Chrzanowska-Wodnicka M, Burridge K (1998). Microtubule depolymerization induces stress fibers, focal adhesions, and DNA synthesis via the GTP-binding protein Rho. Cell Adhes Commun 5, 249–255.
Mücke N, Kirmse R, Wedig T, Leterrier JF, Kreplak L (2005). Investigation of the morphology of intermediate filaments adsorbed to different solid supports. J Struct Biol 150, 268–276.
Osborn M, Weber K (1977). The detergent-resistant cytoskeleton of tissue culture cells includes the nucleus and the microfilament bundles. Exp Cell Res 106, 339–349.
Pelham RJ Jr, Wang Y (1997). Cell locomotion and focal adhesions are regulated by substrate flexibility. Proc Natl Acad Sci USA 94, 13661–13665.
Peyton SR, Putnam AJ (2005). Extracellular matrix rigidity governs smooth muscle cell motility in a biphasic fashion. J Cell Physiol 204, 198–209.
Polioudaki H, Kastrinaki M-C, Papadaki HA, Theodoropoulos PA (2009). Microtubule-interacting drugs induce moderate and reversible damage to human bone marrow mesenchymal stem cells. Cell Prolif 42, 434–447.
Qin Z, Kreplak L, Buehler MJ (2009). Hierarchical structure controls nanomechanical properties of vimentin intermediate filaments. PLoS One 4, e7294.
Raab M, Swift J, Dingal PPCD, Shah P, Shin J-W, Discher DE (2012). Crawling from soft to stiff matrix polarizes the cytoskeleton and phosphoregulates myosin-II heavy chain. J Cell Biol 199, 669–683.
Ridley AJ, Hall A (1992). The small GTP-binding protein Rho regulates the assembly of focal adhesions and actin stress fibers in response to growth factors. Cell 70, 389–399.
Rotsch C, Radmacher M (2000). Drug-induced changes of cytoskeletal structure and mechanics in fibroblasts: an atomic force microscopy study. Biophys J 78, 520–535.
Soellner P, Quinlan RA, Franke WW (1985). Identification of a distinct soluble subunit of an intermediate filament protein: tetrameric vimentin from living cells. Proc Natl Acad Sci USA 82, 7929–7933.
Solon J, Levental I, Sengupta K, Georges PC, Janmey PA (2007). Fibroblast adaptation and stiffness matching to soft elastic substrates. Biophys J 93, 4453–4461.
Strelkov SV, Herrmann H, Aebi U (2003). Molecular architecture of intermediate filaments. Bioessays 25, 243–251.
Tee S-Y, Fu J, Chen CS, Janmey PA (2011). Cell shape and substrate rigidity both regulate cell stiffness. Biophys J 100, L25–7.
Weisenhorn AL, Drake B, Prater CB, Gould Sa, Hansma PK, Ohnesorge F, Egger M, Heyn SP, Gaub HE (1990). Immobilized proteins in buffer imaged at molecular resolution by atomic force microscopy. Biophys J 58, 1251–1258.
Winer JP, Janmey PA, McCormick ME, Funaki M (2009a). Bone marrow-derived human mesenchymal stem cells become quiescent on soft substrates but remain responsive to chemical or mechanical stimuli. Tissue Eng Part A 15, 147–154.
Winer JP, Oake S, Janmey PA (2009b). Non-linear elasticity of extracellular matrices enables contractile cells to communicate local position and orientation. PLoS One 4, e6382.
Yeung T, Georges PC, Flanagan LA, Marg B, Ortiz M, Funaki M, Zahir N, Ming W, Weaver V, Janmey PA (2005). Effects of substrate stiffness on cell morphology, cytoskeletal structure, and adhesion. Cell Motil Cytoskeleton 60, 24–34.